

## THE GEMINI DEEP DEEP SURVEY: III. THE EVOLUTION OF GALAXY STELLAR MASSES

KARL GLAZEBROOK<sup>1</sup>, ROBERTO G. ABRAHAM<sup>2</sup>, PATRICK J. McCARTHY<sup>3</sup>, SANDRA SAVAGLIO<sup>1</sup>, HSIAO-WEN CHEN<sup>4,5</sup>, DAVID CRAMPTON<sup>6</sup>, RICK MUROWINSKI<sup>6</sup>, INGER JØRGENSEN<sup>7</sup>, KATHY ROTH<sup>7</sup>, ISOBEL HOOK<sup>8</sup>, RONALD O. MARZKE<sup>9</sup>, R. G. CARLBERG<sup>2</sup>

*Submitted Jan 4th, 2004*

### ABSTRACT

We present the observed evolution in the stellar mass density locked up in giant galaxies over  $0.8 < z < 2$  measured by the near-infrared selected, spectroscopically complete, Gemini Deep Deep Survey. This is deeper and covers more area than previous surveys and we find a great abundance of massive, old galaxies at  $z >> 1$ . The cosmological mass density in the most massive objects ( $M_\star > 10^{10.8} M_\odot$ ) declines only very slowly to  $z = 2$ . In contradiction to the paradigm of standard hierarchical formation based models, the bulk of the stellar mass in large galaxies was assembled at high redshifts rather than recently. We find no evidence for a dependence of the evolutionary rate on mass, again in contrast with a hierarchical assembly picture. The mass density follows an evolutionary path whose shape agrees well with that independently determined from integration of previous measurements of cosmic star-formation history. This represents the first precision measurement of mass assembly over  $1 < z < 2$  and demonstrates that new ingredients are essential in models of galaxy formation to push back the epoch of star-formation in giant galaxies to higher redshifts.

*Subject headings:* galaxies: evolution

### 1. INTRODUCTION

A fundamental prediction of our current hierarchical paradigm of galaxy formation is that massive galaxies form from an assembly of smaller units (Blumenthal, Faber, Primack, & Rees 1984). In this paradigm the most massive objects form last, driven by the merging history of their dark matter haloes. The model succeeds in describing the appearance of large scale structure, but the evolutionary history of massive galaxies presents problems for this scenario. For example, our Milky Way has not undergone significant mass-building via merging in 10 Gyr (Freeman & Bland-Hawthorn 2002) (although M31 may have, e.g. Ferguson et al. (2002)) and direct observations of the abundance of massive galaxies at  $z = 1$  indicate they are fully formed both in terms of size and stellar mass at this epoch (Lilly et al. 1998; Brinchmann & Ellis 2000; Im et al. 2002).

It is now possible to explore the evolution of galaxy mass beyond  $z = 1$  observationally. Most previous work on the  $z > 1$  universe has concentrated on rest-frame ultraviolet (UV) selected samples for spectroscopic studies (Steidel et al. 1999). The bright UV emission from high star-formation rate (SFR) systems makes it relatively straightforward to secure spectra on 8m class telescopes, but star-formation in galaxies is a stochastic phenomena and correlates poorly with mass (Brinchmann et al. 2003). The most massive galaxies in the

local universe are giant ellipticals and they have very weak UV emission (Lotz, Ferguson, & Bohlin 2000) which makes them difficult to detect at  $z > 1$ . Direct determination of dynamical mass requires spatially resolved velocity measurements of galaxies — this has been done out to  $z = 1$  (Vogt et al. 1997; Gebhardt et al. 2003) but has proved too observationally challenging at higher redshifts due to the signal:noise limitations of resolved studies and lack of suitable instrumentation. It is not clear that the light from galaxies is distributed uniformly enough to provide a reliable velocity probe of the dark halo at  $z > 1$  (Bershady & Andersen 2001).

An alternate approach to probing the mass evolution of galaxies which has come to the fore in recent years is the use of near-infrared (NIR) light, in particular the rest-frame  $K$ -band ( $2.2 \mu\text{m}$ ), as a tracer of the *stellar mass* locked up in galaxies. In the local and  $z < 1$  Universe stellar mass correlates extremely well with dynamical mass (McGaugh et al. 2000; Brinchmann & Ellis 2000). To predict stellar mass evolution galaxy formation models based on cosmological numerical simulations must be augmented with analytical star-formation recipes, (Cole et al. 1994), which is rather computation intensive. Consequently, predictions based on ‘semi-analytic’ models (SAM) that adopt simplified prescriptions for various heating and cooling processes in interstellar medium (ISM) dominate the theoretical aspect of the field (Kauffmann & Charlot 1998; Baugh et al. 2003).

The  $K$ -band light in galaxies is dominated by the old, evolved stellar populations in galaxies and is little affected by transient star-formation (Rix & Rieke 1993). To a good approximation the total  $K$ -band light traces the accumulation of stellar mass; equivalently one can say that the stellar mass-to-light ratio ( $M/L$ ) is nearly constant with little dependence on the previous star-formation history (SFH). In fact  $M/L_K$  varies only  $\times 2$  between extremely young and extremely old galaxy spectral energy distributions (SEDs), while  $M/L_B$  can vary by more than a factor of 10 (Bell et al. 2003). The ultraviolet  $M/L$  varies tremendously, because the UV light is dominated by the instantaneous SFR (e.g. Glazebrook et al. (1999)) rather than the total stellar mass and can reach values as low as 1%. Moreover the shape of rest-frame NIR

<sup>1</sup> Department of Physics & Astronomy, Johns Hopkins University, 3400 North Charles Street, Baltimore, MD 21218-2686.

<sup>2</sup> Department of Astronomy & Astrophysics, University of Toronto, 60 St. George Street, Toronto, ON, M5S 3H8, Canada

<sup>3</sup> Observatories of the Carnegie Institute of Washington, Santa Barbara Street, Pasadena, CA 91101

<sup>4</sup> Center for Space Research, Massachusetts Institute of Technology, Cambridge, MA 02139-4307

<sup>5</sup> Hubble Fellow

<sup>6</sup> Herzberg Institute of Astrophysics, National Research Council, 5071 West Saanich Road, Victoria, British Columbia, V9E 2E7, Canada.

<sup>7</sup> Gemini Observatory, Hilo, HI 96720

<sup>8</sup> Department of Astrophysics, Nuclear & Astrophysics Laboratory, Oxford University, Keble Road, Oxford OX1 3RH, U.K.

<sup>9</sup> Dept. of Physics and Astronomy, San Francisco State University, 1600 Holloway Avenue, San Francisco, CA 94132

galaxy spectra are almost independent of star-formation history. Thus observed-frame  $K$ -band selection and mass estimates remain robust out to  $z \sim 2$ ; it is only for  $z \gtrsim 3$  when the light below 5000Å enters the  $K$ -band that this relationship begins to break down (Mannucci et al. 2001).

Observations of the galaxy stellar mass function (GSMF) via  $K$ -band light represent an alternate way of viewing Universal star-formation as a function of redshift which has previously been determined from the UV (Madau et al. 1996; Lilly, Le Fevre, Hammer, & Crampton 1996; Steidel et al. 1999) of cosmic SFR- $z$ . Broadly speaking, the integral of cosmic SFR over time must correspond to the accumulated stellar mass density. Since these are measured in completely different ways (e.g. UV luminosity density and  $H\alpha$  for SFR; Glazebrook et al. (1999)) they represent independent constraints on cosmic stellar evolution. The UV SFR measurements appear to indicate that at least 50% of the stellar mass in galaxies formed over  $1 < z < 2$ ; a regime we can now probe observationally. A notable point is that  $K$ -band measurements of mass are largely unaffected by dust, firstly because the NIR is intrinsically less extinguished, and secondly because long-lived evolved stars no longer occupy dusty regions. This contrasts with UV SFR measurements where the dust correction is a factor of  $\sim 6$  upwards, and represents a considerable uncertainty (Steidel et al. 1999).

The MUNICS survey (Drory et al. 2001) has estimated the galaxy stellar mass function (GSMF) tip at  $z = 1$  from a  $K < 19$  photometric redshift ('photo-z') sample (calibrated with  $K < 17$  redshifts) and find some evidence of growth since  $z = 1$ . Bell et al. (2003) infer a  $\times 2$  growth in stellar mass since  $z \sim 1.3$  from their photometric analysis of the COMBO-17 survey. Dickinson et al. (2003) has estimated the evolution of the integrated GSMF (which is equivalent to  $\Omega_*$ ) at  $z > 1$  using deep  $K$ -band imaging and photometric redshifts of the Hubble Deep Field (HDF) North. They found broad agreement of  $\Omega_*(z)$  measured with that inferred from the integration of UV-derived cosmic SFH (though see below); however this suffered from a very small sky area (5 arcmin<sup>2</sup>) and did not cover the  $1 < z < 2$  region well. At  $z = 2.7$  Dickinson et al. measure a stellar mass density that is only 10-15% of the present value. Fontana et al. (2003) used a similar photometric approach in the HDF South and found twice as many massive galaxies, in excess of SAM predictions, but the HDF-N comparison highlighted the large cosmic variance associated with such small survey areas.

In this paper we present the evolution in the galaxy stellar mass function determined from the Gemini Deep Deep Survey, which covers a much larger area than previous studies, samples multiple sight-lines and identifies massive galaxies spectroscopically to  $z \lesssim 2$ . Throughout we adopt a cosmology of  $\Omega_\Lambda = 0.7$ ,  $\Omega_M = 0.3$  and  $H_0 = 70 \text{ km s}^{-1} \text{ Mpc}^{-1}$ .

## 2. METHODS

The Gemini Deep Deep Survey (GDDS) is an infrared-selected ( $K < 20.6$  mag) ultra-deep spectroscopic survey of  $0.8 < z < 2$  galaxies. The GDDS sample selection, experimental design and catalog are described in great detail in Abraham et al. (2004) ('Paper I') and will only be described briefly here. The primary sample was drawn from the 1-square degree Las Campanas Infrared Survey (McCarthy et al. 2001; Chen et al. 2003) and consisted of galaxies with  $K < 20.6$  and  $I < 24.5$  selected with photometric redshift cuts to exclude most of the  $z < 0.8$  foreground (in the  $z < 1$  regime the photometric redshifts are extremely reli-

able; Chen et al. (2003)). At  $I < 24.5$  mag the selection is virtually color complete even for the reddest  $K$ -selected galaxies (only 10 of the  $K < 20.6$  galaxies in our entire survey area have  $I > 24.5$ ). Spectra of 301 galaxies were obtained in four 30 arcmin<sup>2</sup> fields. Exposures of  $> 30$  hours per field were taken using the 8.1m Gemini North telescope using the 'nod & shuffle' sky-removal technique (Glazebrook & Bland-Hawthorn 2001) to secure optical spectra good enough for redshift identification (79% completeness) and spectral classification. Galaxies with colors and spectra of both old and young stellar populations are identified out to  $z \simeq 1.8$ . Example spectra of old systems are presented in Paper I (Abraham et al. 2004) and Paper IV (McCarthy et al. 2004), while examples of blue galaxy spectra are shown in Paper II (Savaglio et al. 2004).

The sample used here is based on Table 4 of Paper I, to which the reader is referred for details. We only consider galaxies with redshifts between  $0.5 < z < 2$  (240 galaxies). For galaxies with redshift confidence classes  $\geq 2$  (88% of the sample in this redshift range), we adopt the spectroscopic redshifts in Table 4; for the remainder (12% of the sample) with either no redshifts or very low-confidence redshifts, we use the LCIRS photometric redshift as derived by Chen et al. The core sample for the mass function analysis has  $K < 20.6$  and  $0.8 < z < 2$  (150 galaxies; 89% spectroscopic completeness); as described in Paper I, the GDDS was designed around this magnitude limit and redshift range.

The sampling of galaxies in the GDDS is not completely homogeneous in the sense that when designing spectroscopic masks a higher priority was given to red galaxies than to blue galaxies. To account for this, Paper I gives 'sampling weights', which are the spectroscopic selection probability as a function of  $I - K$  and  $K$ . These are referenced to the full wide-area LCIRS fields and so also account approximately for the effect of cosmic variance. We also note that the GDDS survey areas were selected as be neither particularly under or over-dense in highly clustered red objects (Daddi et al. 2003; McCarthy et al. 2001).

For each galaxy we derive the most likely stellar mass and a range of uncertainty. These are derived from fitting model spectral-energy distributions (SED) to the galaxy optical-IR colors in order to determine the  $M/L_K$  ratio, and hence the mass. We note that a variety of approaches to accomplish this have been described in the literature (e.g. Brinchmann & Ellis (2000) which vary in the level of detail in which they treat star formation. For example, Cole et al (2001) used a simple set of monotonic star-formation histories with a varying e-folding timescale and a fixed dust law. A potential problem is posed by the fact that real galaxies have more complex SFHs, for example a recent starburst can make an old galaxy temporarily bluer and lead to an underestimate of  $M/L$  using this method. One approach to attempt to account for this is to introduce a second young SED component (e.g. Fontana et al. (2003)) superimposed on the old population; this can be computationally expensive depending on the amount of freedom allowed for the second component.

In a spectroscopic sample there is no degeneracy between SED model fitting and photometric redshift (which is also based on SED fitting). We adopt two-component fitting (using PEGASE.2 (Fioc & Rocca-Volmerange 1997) to calculate spectra) in order to be able to assess the possible biases due to starbursts on the calculated masses and allow a range of dust extinction ( $0 \leq A_V \leq 2$  mag) and metallicity ( $0.0004 \leq Z \leq 0.02$ ). The primary component is modeled

using  $SFR \propto \exp(-t/\tau)$  with  $\tau = 0.1, 0.2, 0.5, 1, 2, 4, 8$  & 500 Gyr. (The first approximates an instantaneous starburst and the last a constant SFR). The secondary component is a starburst, modeled with a  $\tau = 0.1$  Gyr exponential, which can occur at any time and have a mass between  $10^{-4}$  and twice that of the parent. We use the Baldry & Glazebrook (2003) Initial Mass Function (IMF) which has the same high-mass slope as Salpeter (1955) (thus fitting galaxy colors well), but which has a break at  $1 M_\odot$  (providing more realistic  $M/L$  values).<sup>10</sup>

We fit the model spectra to the  $VIZ'K$  photometry in the observed frame of each galaxy. This color set is available for all galaxies and covers rest-frame UV-NIR. We do not include the actual spectra (apart from the redshift information) in the fits because of variable quality and signal:noise<sup>11</sup>. Monte Carlo simulations based on the photometric errors were used to calculate distributions of best fitting parameters. Full details of this methodology will be given in a future paper, where we will explore the distribution functions and mutual dependence of fitted parameters (including masses, SFRs and burst strengths). At present we wish only to emphasize that the stellar masses are robust against all these details. Typically, we find the masses are fitted to  $\pm 0.17$  dex in the  $K < 20.6$  sample. Using the fitting machinery to investigate the effect of different assumptions about metallicity, dust and bursts we find that the largest effect is due to bursts. If we disallowed bursts then the masses typically decrease by only 0.2 dex. In fact we find qualitatively the same scientific results even if we assume  $M/L_K$  to be a *constant*; the findings presented below are simply driven by the presence of numerous  $K \sim 20$  galaxies at  $z > 1.5$ .

### 3. RESULTS

We begin our discussion of the results from the GDDS by showing two plots which show where the massive galaxies occur in redshift/color/ $K$  space. Figures 1 and 2 shows the mass and observed  $I - K$  color of our sample as a function of redshift. Symbol sizes and colors in Figure 1 are keyed to  $I$ -band and  $K$ -band magnitude, respectively. In Figure 2 symbol sizes are keyed to mass, and symbol colors are keyed to spectral classification (using the system defined in Paper I).

The following trends are apparent from these figures:

1. The GDDS identifies massive galaxies to  $z = 2$ , even when they are very red ( $I - K > 4$ ). For comparison, the local galaxy characteristic mass ( $M^*$  in a Schechter (1976) function) is plotted in Figure 1; this is  $10^{10.9} M_\odot$  (the value in Cole et al. 2003 converted to our cosmology & IMF).
2. At  $z > 1$  there is an increasing abundance of blue galaxies. Some of these are quite massive and are discussed in Paper II. However 60% of the mass at  $1.2 < z < 1.8$  is in objects with colors redder than a Scd (star symbols in Figure 2).

<sup>10</sup> To a good approximation  $M/L_K(BG) = 0.55M/L_K(SP)$  (accurate to a few percent independently of the SFH). Similarly SFR(BG03 for const. UV) =  $0.52 \times$  SFR(SP for const. UV) on average (with only a 1.5% variation over 1500Å–2000Å). Thus using the BG03 IMF facilitates easy comparison with Salpeter based analyses while being more physically motivated than, for example, the ‘diet-Salpeter’ IMF of Bell et al. (2003).

<sup>11</sup> In GDDS Paper IV (McCarthy et al. 2004) we investigate fitting the spectra and photometry both together and separately for the best spectra

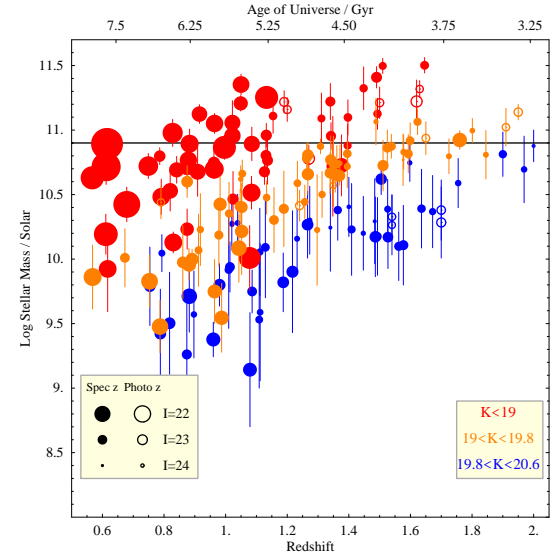


FIG. 1.— Mass-redshift relation for GDDS galaxies, showing the errors on the mass fitting and color coded by observed  $K$ -magnitude. Solid circles and open circles denote spectroscopic and photometric redshifts respectively. Symbol size is keyed to the  $I$ -band magnitude. The horizontal line denotes  $M^*$  at  $z = 0$  from Cole et al.

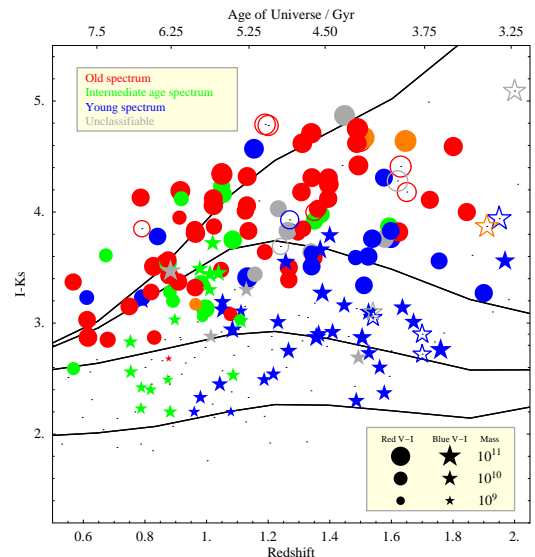


FIG. 2.— Observed frame  $I - K$  colors of GDDS galaxies vs redshift for the  $K < 20.6$  sample. The symbol size is keyed to the mass. The symbol shape is keyed to optical  $V - I$  color (circles are redder than a model Coleman, Wu, & Weedman (1980) Sbc template at each redshift) and the symbol color is keyed to the spectral classification. Open symbols are photometric redshifts. Model tracks are shown for passive evolution through to const. SFR, for synthetic galaxies which form at  $z = 10$ .

3. There is a large contribution to the stellar mass from galaxies which our spectra confirm have old stellar populations. These are the systems classed as 001 and 011 in the system defined in Paper I, and are shown using red symbols in Figure 2. They are not simply red due to dust; photospheric features from evolved stars are seen in their spectra, confirming that genuine old stellar populations dominate this population (see Paper IV for more details on this). At  $1.2 < z < 1.8$  25% of the mass is locked up in these systems.

We next compute the cumulative mass density per unit vol-

ume in each redshift bin down to various mass thresholds, following the standard  $V_{max}$  formalism for a  $K < 20.6$  limit, and using the weights from Paper I (which are normalized to 554.7 arcmin $^2$ ). We use K-corrections from our individual SED fits, but find the results are identical if we use different K-corrections.

The cumulative mass density as a function of redshift and mass limit is plotted in Figure 3 and tabulated in Table 1. Although a  $K$ -selected sample is a good proxy for a mass-selected sample, it is still necessary to consider incompleteness as a function of  $M/L$ . To do this we compute the maximum possible  $M/L$  at each redshift for a model galaxy as old as the Universe which formed all its stars at once. This  $M/L$  is converted to a mass limit via the  $K = 20.6$  limit and the K-correction. This limit is  $\log(M/M_\odot) = 10.10, 10.30, 10.45, 10.70$  for  $z = 1.1, 1.3, 1.6, 2$ . The reddest possible objects are only visible for bins with masses above these limits. Objects which are bluer (lower  $M/L$ ) can be seen to a lower mass than these limits. Since the particular bins which encompass these limits may be missing red objects the calculated densities are plotted as *lower limits* in Figure 3. The error bars are calculated from shot noise on the number of galaxies in each bin. We have assessed the effect of the mass fitting errors on the mass densities with our Monte-Carlo methods; this is not a significant source of error. In every bin spectroscopic redshifts dominate the mass budget except only for the  $1.6 < z < 2$  and  $M > 10^{10.8} M_\odot$  bin where 50% of the redshifts are photometric. However even if we re-analyze the entire sample throwing out all photometric redshifts the same scientific result is obtained. We have also checked the effect of cosmic variance (very important for red galaxies which are highly clustered; McCarthy et al. (2001) by splitting the sample in to two using different fields; the mass density results are always consistent with each other and the total sample. This agrees with tests we have made drawing sample GDDS surveys from the LCIRS catalogs.

The fundamental finding from the data in Figure 3 is that the mass density in large galaxies declines only slowly at high-redshift. At  $z = 1$  the mass densities are about 80% of their local value; at  $z = 2$  this becomes 30%. Overlaid on Figure 3 (shaded region) is the range of estimates for the growth of total stellar mass based on the integral (using PEGASE.2) of the observed SFR- $z$  relationship. These are based on the points from Figure 9 of Steidel et al 1999 using the analytic fit of Cole et al. (2001) with and without extinction correction. We confirm the result of Cole et al. (2001) that an extinction correction is essential for UV SFR estimates to be consistent with stellar mass measurements; we have now extended this finding from the local Universe to  $z = 2$ . Given this dust correction the shape of the decline of stellar mass is in good agreement with the UV prediction and it is independent of the mass cut. However it is possible from our data that the mass density could be still higher indicating that UV selection could miss some of the SFR at  $z > 2$  (see Franx et al. (2003) for findings along this line). In our own sample UV selection certainly misses a lot of the mass which must then form at higher redshift.

We also plot the predictions from a fairly standard semi-analytic model (SAM) of hierarchical galaxy formation converted to our IMF. We choose the GALFORM models (Granato et al. 2000; Baugh et al. 2003) as representing the paradigm of late formation; these reproduce many features of the local Universe and show the standard trend where the higher mass galaxies disappear much faster at higher redshift.

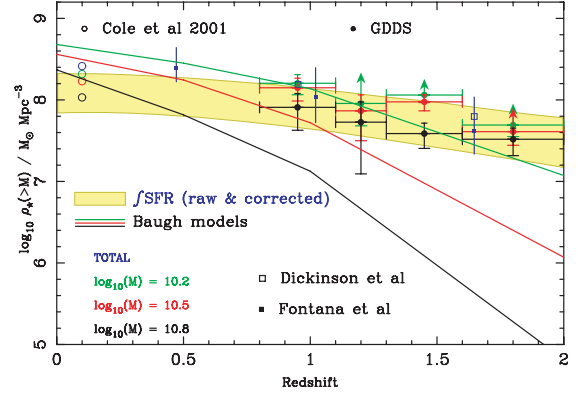


FIG. 3.— Mass density vs redshift for GDDS galaxies (solid circles) at  $z \gtrsim 1$  and from Cole et al. (2001) (open circles) in the local Universe (we take  $\bar{z} = 0.1$ ). We plot the cumulative mass density of galaxies more massive than a given mass threshold. Photometric estimates of the total mass density from Fontana et al. (2003) and Dickinson et al. (2003) which are claimed to be total are also plotted (filled squares; open squares). The solid lines show the same quantity from the GALFORM model. The shaded region shows the result of integrating the Universal UV-derived SFH without and with a dust correction.

From this comparison we conclude the following:

1. Massive galaxies ( $\gtrsim 10^{10.5} M_\odot$ ) are still quite abundant at  $z > 1.6$  in contradiction with this model.
2. The rate of evolution appears to be independent of mass: giant galaxies decline at the same, slow, rate as the smaller ones, again in disagreement with this model.
3. We note that the GALFORM models displayed here considerably overshoot the local measured mass density in order to get the  $z \sim 1$  mass density approximately right. If the models were to be normalized to match the local mass density at  $z = 0$  they would fail to match our data even at  $z = 1$ . Clearly at  $z > 1$  the problem with the most massive galaxies becomes rather worse and more difficult to reconcile with the data.

The simplest model that matches our data for giant galaxies is early formation of a large fraction of the stellar constituents followed by modest additional growth. This is at odds with the paradigm of late formation. The evidence from galaxy clustering locally (Percival et al. 2001) and from the Cosmic Microwave Background at high redshift (Spergel et al. 2003) strongly support the basic  $\Lambda$ CDM picture, which seems to correctly explain the abundance and clustering of dark matter haloes. (However see McGaugh (2004) for an alternative point of view). Is there a paradox? The answer is ‘probably not’, because failures in these particular models do not necessarily imply a failure in  $\Lambda$ CDM; the total baryon mass budget is not violated.<sup>12</sup> As we lack a general model for star formation in galaxies, the problem probably lies in the analytical prescription used in converting baryons into stars. Some way has to be found to make star-formation more efficient at early times for the more massive galaxies to counteract the increasing scarcity of their haloes. Improved hydrodynamic simulations incorporating more sophisticated treatment

<sup>12</sup> The space density of  $> 10^{11} M_\odot$  (stellar mass)  $z > 1.6$  GDDS galaxies is about  $2 \times 10^{-4} \text{ Mpc}^{-3}$ . The predicted abundance of  $> 10^{12} M_\odot$  (dark matter mass)  $z = 2$  CDM haloes (which would contain enough baryons) is about 5× higher (Sheth & Tormen 1999)

in the ISM physics (Springel & Hernquist 2003; Hernquist & Springel 2003) have in fact predicted that within the framework of  $\Lambda$ CDM models as much as 70% of the total stellar mass density was already in place by  $z=1$  (Negamine et al. (2004); also see Gao et al. (2004) and Somerville, Primack, & Faber (2001)). We note that a similar mechanism may be needed to explain the sizes of high-redshift disks, c.f. Lilly et al. (1998) but they must avoid making  $z > 1$  galaxies too blue (Somerville et al. 2003; Stanford et al. 2004). Such mechanisms can be probably be found. However, we also point out that our data would be compatible with a non-hierarchical picture, simply because the observed galaxy evolution is independent of mass.

What is clear is that we have spectroscopically identified a  $z \sim 2$  population, already mostly assembled, which is a very plausible precursor of current day massive elliptical galaxies. Late formation is ruled out (in contradiction for example with Zepf (1997)). An unresolved question is what do these become at still higher redshifts? There must be a yet undiscovered epoch of formation when these massive old galaxies *did* assemble. The known high- $z$  high-SFR sources do not appear to suffice.  $z \sim 3$  Lyman break galaxies do not appear massive enough (Papovich, Dickinson, & Ferguson 2001) and the sub-mm sources peak at  $z = 2$  (Chapman, Blain, Ivison, & Smail 2003) which is too close in time. In any case, it is clear that the increasing wealth of data from sources such as the Gemini Deep Deep Survey will drive increasingly sophisticated models of galaxy evolution.

Based on observations obtained at the Gemini Observatory, which is operated by AURA under a cooperative

agreement with the NSF on behalf of the Gemini partnership: NSF (U.S.), PPARC (U.K.), NRC (Canada), CONICYT (Chile), ARC (Australia), CNPq (Brazil) and CONICET (Argentina). Karl Glazebrook & Sandra Savaglio acknowledge generous funding from the David and Lucille Packard Foundation. Hsiao-Wen Chen acknowledges support by NASA through a Hubble Fellowship grant HF-01147.01A from the Space Telescope Science Institute, which is operated by the Association of Universities for Research in Astronomy, Incorporated, under NASA contract NAS5-26555

TABLE 1  
GALAXY STELLAR MASS DENSITY MEASUREMENTS

$\log M_{lim}$	$z$ range	$\log \rho$	$\log \rho_{lo}$	$\log \rho_{hi}$	Complete?
10.2	0.8–1.1	8.20	8.06	8.31	Y
10.2	1.1–1.3	7.96	7.68	8.12	N
10.2	1.3–1.6	8.06	7.97	8.14	N
10.2	1.6–2.0	7.69	7.55	7.80	N
10.5	0.8–1.1	8.15	7.99	8.27	Y
10.5	1.1–1.3	7.87	7.50	8.06	Y
10.5	1.3–1.6	7.98	7.87	8.06	Y
10.5	1.6–2.0	7.61	7.44	7.73	N
10.8	0.8–1.1	7.91	7.63	8.08	Y
10.8	1.1–1.3	7.73	7.09	7.97	Y
10.8	1.3–1.6	7.59	7.41	7.72	Y
10.8	1.6–2.0	7.52	7.32	7.65	Y

Units of  $\rho$  are  $M_{\odot} \text{ Mpc}^{-3}$  and are for  $h = 0.7$ . Multiply masses by 1.82 to convert BG03 IMF to Salpeter.

## REFERENCES

Abraham, R. G. et al. 2004, AJ submitted [Paper I]  
 Baldry, I. K. & Glazebrook, K. 2003, ApJ, 593, 258  
 Baugh, C. M., Benson, A. J., Cole, S., Frenk, C. S., & Lacey, C. 2003, The Mass of Galaxies at Low and High Redshift, 91  
 Bell, E. F., McIntosh, D. H., Katz, N., & Weinberg, M. D. 2003, ApJS, 149, 289  
 Bershady, M. & Andersen, D. R. 2001, ASP Conf. Ser. 230: Galaxy Disks and Disk Galaxies, 589  
 Blumenthal, G. R., Faber, S. M., Primack, J. R., & Rees, M. J. 1984, Nature, 311, 517  
 Brinchmann, J. & Ellis, R. S. 2000, ApJ, 536, L77  
 Brinchmann, J. et al. 2003, ApJ, in press (astro-ph/0311060)  
 Chapman, S. C., Blain, A. W., Ivison, R. J., & Smail, I. R. 2003, Nature, 422, 695  
 Chen, H.-W. et al. 2003, ApJ, 586, 745  
 Cole, S., Aragon-Salamanca, A., Frenk, C. S., Navarro, J. F., & Zepf, S. E. 1994, MNRAS, 271, 781  
 Cole, S. et al. 2001, MNRAS, 326, 255  
 Coleman, G. D., Wu, C.-C., & Weedman, D. W. 1980, ApJS, 43, 393  
 Daddi E. et al. 2003, ApJ, in press (astro-ph/0308456)  
 Dickinson, M., Papovich, C., Ferguson, H. C., & Budavári, T. 2003, ApJ, 587, 25  
 Drory, N., Bender, R., Snigula, J., Feulner, G., Hopp, U., Maraston, C., Hill, G. J., & de Oliveira, C. M. 2001, ApJ, 562, L111  
 Ferguson, A. M. N., Irwin, M. J., Ibata, R. A., Lewis, G. F., & Tanvir, N. R. 2002, AJ, 124, 1452  
 Fioc, M. & Rocca-Volmerange, B. 1997, A&A, 326, 950  
 Fontana, A. et al. 2003, ApJ, 594, L9  
 Franx, M. et al. 2003, ApJ, 587, L79  
 Freeman, K. & Bland-Hawthorn, J. 2002, ARA&A, 40, 487  
 Gao et al. 2004, ApJ, submitted (astro-ph/0312499)  
 Gebhardt, K. et al. 2003, ApJ, 597, 239  
 Glazebrook, K., Peacock, J. A., Miller, L., & Collins, C. A. 1995, MNRAS, 275, 169  
 Glazebrook, K., Blake, C., Economou, F., Lilly, S., & Colless, M. 1999, MNRAS, 306, 843  
 Glazebrook, K. & Bland-Hawthorn, J. 2001, PASP, 113, 197  
 Granato, G. L., Lacey, C. G., Silva, L., Bressan, A., Baugh, C. M., Cole, S., & Frenk, C. S. 2000, ApJ, 542, 710  
 Hernquist, L. & Springel, V. 2003, MNRAS, 341, 1253  
 Im, M. et al. 2002, ApJ, 571, 136  
 Kauffmann, G. & Charlot, S. 1998, MNRAS, 297, L23  
 Lilly, S. J., Le Fevre, O., Hammer, F., & Crampton, D. 1996, ApJ, 460, L1  
 Lilly, S. et al. 1998, ApJ, 500, 75  
 Lotz, J. M., Ferguson, H. C., & Bohlin, R. C. 2000, ApJ, 532, 830  
 Madau, P., Ferguson, H. C., Dickinson, M. E., Giavalisco, M., Steidel, C. C., & Fruchter, A. 1996, MNRAS, 283, 1388  
 Mannucci, F., Basile, F., Poggianti, B. M., Cimatti, A., Daddi, E., Pozzetti, L., & Vanzi, L. 2001, MNRAS, 326, 745  
 McCarthy, P. J. et al. 2001, ApJ, 560, L131  
 McCarthy et al. 2004, ApJ, in preparation  
 McGaugh, S. S. 2004, ApJ, submitted (astro-ph/0312570)  
 McGaugh, S. S., Schombert, J. M., Bothun, G. D., & de Blok, W. J. G. 2000, ApJ, 533, L99  
 Negamine, K., Cen, R., Hernquist, L., Ostriker, J. P., & Springel, V. 2004, ApJL submitted (astro-ph/0311294)  
 Papovich, C., Dickinson, M., & Ferguson, H. C. 2001, ApJ, 559, 620  
 Percival, W. J. et al. 2001, MNRAS, 327, 1297  
 Rix, H. & Rieke, M. J. 1993, ApJ, 418, 123  
 Salpeter, E. E. 1955, ApJ, 121, 161  
 Savaglio et al. 2004, ApJ, in press, (ast ro-ph/031043), [Paper II]  
 Sheth, R. K. & Tormen, G. 1999, MNRAS, 308, 119  
 Somerville, R. S., Primack, J. R., & Faber, S. M. 2001, MNRAS, 320, 504  
 Somerville, R. S. et al., 2003, ApJ, in press  
 Spergel, D. N. et al. 2003, ApJS, 148, 175  
 Springel, V. & Hernquist, L. 2003, MNRAS, 339, 289  
 Stanford S. A., et al., 2004, ApJ, in press (astro-ph/0310231)  
 Steidel, C. C., Adelberger, K. L., Giavalisco, M., Dickinson, M., & Pettini, M. 1999, ApJ, 519, 1  
 van den Bergh, S., Abraham, R. G., Ellis, R. S., Tanvir, N. R., Santiago, B. X., & Glazebrook, K. G. 1996, AJ, 112, 359  
 Vogt, N. P. et al. 1997, ApJ, 479, L121  
 Zepf, S. E. 1997, Nature, 390, 377